**HEFAT2012**
**9th International Conference on Heat Transfer, Fluid Mechanics and Thermodynamics**
**16 – 18 July 2012**
**Malta**

# DESTABILIZATION OF FREE CONVECTION BY WEAK ROTATION

Gelfgat A.Y.*
*Author for correspondence
School of Mechanical Engineering, Faculty of Engineering,
Tel-Aviv University,
Ramat Aviv, Tel-Aviv, 69978,
Israel,
E-mail: gelfgat@tau.ac.il

## ABSTRACT

In the present study we seek an explanation of several recent observations of steep destabilization of convective flow in Czochralski crystal growth models by a slow rotation of the crystal. Existing experimental and computational evidence shows that destabilization takes place in a wide range of the Prandtl number, from semiconductor melts with $Pr\sim10^{-2}$ up to experiments with very viscous silicone oils having $Pr\sim10^{3}$. Examination of several models where flows are driven by the simultaneous action of convection and rotation shows that the destabilization is observed in cases where centrifugal force acts against main convective circulation. This allows us to choose a generic model, which is flow in a cylinder with parabolic temperature profile at the sidewall and rotating top, exhibiting the destabilization for a wide range of the Prandtl numbers. Further observation of the flow and disturbance patterns shows that at relatively low Prandtl numbers the counter action of buoyancy and centrifugal forces can split the main vortex into two counter rotating vortices, whose interaction leads to instability. At larger Prandtl numbers the counter action of the centrifugal force steepens an unstable thermal stratification, which triggers the Rayleigh-Bénard instability mechanism.

## INTRODUCTION

This paper briefly describes an effect of destabilization of axisymmetric natural convection flows by a weak superimposed non-uniform rotation. In classical models, such as a rotating infinite layer or rotating cylinders and annuli, increasing rotation usually leads to stabilization of the flow, i.e., to the growth of the critical Rayleigh number or other critical parameters describing magnitude of the buoyancy force (see, e.g., [1,2] and references therein). These results lead to an intuitive expectation of a stabilizing effect of rotation on convective instabilities. However, such an expectation is generally wrong. The two above models consider classical Rayleigh-Bénard problem of stability of purely conducting quiescent states, while in most practically important cases, the buoyancy force is non-potential, so that natural convection flow always exists. Reviewing several studies devoted to instabilities driven by the simultaneous effect of convection and rotation, Koschmieder [2] noted that when the rotation affects the base flow, its effect on flow instability becomes very complicated. We can add that non-uniform rotation caused by a rotating boundary or an external force complicates the stability properties of flows even more. This was observed, for example, by Brummel [3] and Ali & McFadden [4].

This study is motivated by several recent observations of destabilization of convective flow by rotation in models of Czochralski bulk crystal growth process [5]. These models consider melt flow in a cylindrical crucible with a heated bottom and sidewall, cooled by a rotating cold crystal pulled out from the upper free surface. In laboratory flow models, the crystal is usually replaced by a cooled cylindrical dummy whose lower surface touches the free surface of working liquid. Rotation and lower temperature of the dummy mimic the effect of the crystal in a technological setup [6-8]. The flow is driven by buoyancy, rotation of the crystal and thermocapillary force acting along the free surface. Stability studies of these flows focus on parameters at which steady – oscillatory flow transition takes place. Different examples can be found in [9] and references therein. Figure 1 shows two examples of stability diagrams, in which critical temperature difference $\Delta T_{cr}$, to which both Grashof and Marangoni numbers are proportional, is plotted versus the Reynolds number defined by the angular velocity of the dummy rotation and the crucible radius. The system geometry and an example of the flow pattern are shown in the insert. Further details can be found in [8-10]. Both examples relate to similar experiments with different working liquids with the Prandtl number $Pr$=9.2 in the case (a) of Schwabe *et al.* [7] and $Pr$=23.9 in the case (b) of Teitel *et al.* [8]. In both examples computations predict a steep decrease of $\Delta T_{cr}$ with a slow increase of the rotational Reynolds number up to $Re$=100, which corresponds to the rotation of crystal with the angular viscosity smaller than 0.1 and 0.5 rad/s

(1 and 5 revolutions per minute) in the cases (a) and (b), respectively. Note that depending on the aspect ratio, isothermal swirling flow in a cylinder with a rotating lid becomes unstable for the Reynolds number between 2000 and 3000 [13], so that the destabilization observed in Fig. 1a,b cannot be addressed to a rotation-induced instability. Note also that in spite of the critical temperature difference $\Delta T_{cr}$ decreases in more than an order of magnitude, it never reaches zero. Therefore, it is an interaction of all the driving forces that makes the flow significantly lesser stable. It should be emphasized also that destabilization was observed also experimentally and numerically in low-Prandtl-number semiconductor melts, so that the explanation(s) of the whole phenomena must relate to a very wide range of the Prandtl number (see [11] for details).

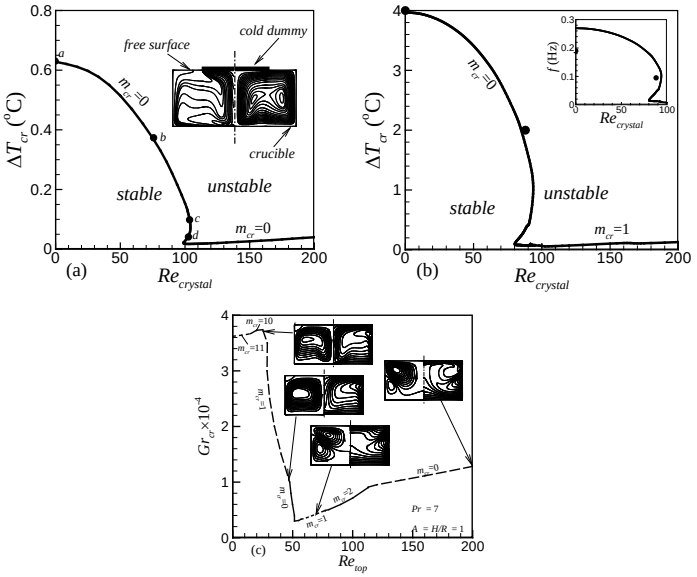


**Figure 1** Neutral stability curves for two models of Czochralski melt. (a) – configuration Schwabe *et al*. (2004); the insert shows the streamlines (right frame) and isotherms (left frame) at $\Delta T$=0.5. (b) configuration of Teitel *et al.* (2008); symbols correspond to experimentally measured critical points, the insert shows frequency of flow oscillations at the critical points (curve) and experimentally measured frequencies. (c) Neutral stability curve of flow in a cylinder with parabolic temperature profile at the sidewall and rotating top at *Pr*=7. Inserts show streamline (left) and isotherm (right) patterns at different points of the neutral curve.

Since the Czochralski flow model is rather complicated, in the present study we are looking for a simpler characteristic model exhibiting similar destabilization and intend to study the latter to get more physical insight in the phenomenon. Considering several examples of flows driven by convection and rotation we arrived to the conclusion that the simplest model exhibiting similar destabilization is a combination of two well-studied cases: convective flow in a vertical cylinder with a parabolic temperature profile at the sidewall, and swirling flow in a cylinder with a rotating lid. The three-dimensional stability of the first one was studied in [12] and of the second one in [13]. The stability diagram corresponding to the combination of the two cases at *Pr*=7 is shown in Fig. 1c, where at *Re*=50 the critical Grashof number decreases in more than an order of magnitude. Examining the flow and leading disturbance patterns we arrive at a conclusion that destabilization is caused by a counter action of the centrifugal force that tends to slow down the main convective vortex. This counter action leads either to the appearance of a new vortical structure, which is characteristic to small Prandtl numbers, or to a steeper temperature gradient along the axis observed at larger *Pr*. Consequently, the following destabilization is connected either to an interaction between counter rotating vortices ($Pr \lesssim 1$), or to the Rayleigh-Bénard instability developing below the cold upper boundary ($Pr \gtrsim 1$). An additional destabilization mechanism is connected to the advection of perturbations of azimuthal velocity towards the axis, where they grow due to conservation of the angular momentum, which causes a growth of the radial velocity disturbances. In this short paper we focus mostly on the cases with a relatively large Prandtl number, for which the instability, as well as destabilization, are caused by an unstable stratification below the cold upper cylinder boundary.

## FORMULATION OF THE PROBLEM

We study three-dimensional instabilities of axisymmetric non-isothermal base flows. The full three-dimensional problem is described by the Boussinesq equations in cylindrical coordinates. A Boussinesq fluid with density $\rho^*$, kinematic viscosity $\nu^*$ and thermal diffusivity $\chi^*$ in an axisymmetric region $0 \le r \le R^*$, $0 \le z \le H^*$ is considered. The polar axis is assumed to be parallel to the gravity force. The flow is described by the momentum, continuity and energy equations in cylindrical coordinates $(r^*, z^*)$. To render the equations dimensionless, we use the scales $R^*$, $R^{*2}/\nu^*$, $\nu^*/R^*$, $\rho^*(\nu^*/R^*)^2$ for length, time, velocity and pressure respectively. The temperature is rendered dimensionless by the relation $T = (T^* - T^*_{cold})/(T^*_{hot} - T^*_{cold})$, where $T^*_{hot}$ and $T^*_{cold}$ are the maximal and minimal temperatures at the boundaries of the flow region. The set of Boussinesq equations for the non-dimensional velocity $\mathbf{v} = \{v_r, v_\theta, v_z\}$, temperature $T$ and pressure $p$ in the domain $0 \le r \le 1$, $0 \le z \le A$ reads

$$\frac{\partial \mathbf{v}}{\partial t} + (\mathbf{v}\cdot\nabla)\mathbf{v} = -\nabla p + \Delta\mathbf{v} + GrT\,\mathbf{e}_z \qquad (1)$$

$$\frac{\partial T}{\partial t} + (\mathbf{v}\cdot\nabla)T = \frac{1}{Pr}\Delta T, \qquad \nabla\cdot\mathbf{v} = 0 \qquad (2,3)$$

Here $A = H^*/R$ is the aspect ratio, $Gr = g^*\beta^*(T^*_{hot} - T^*_{cold})R^{*3}/\nu^{*2}$ the Grashof number, $Pr = \nu^*/\chi^*$ the Prandtl number, $g^*$ gravity acceleration, $\beta^*$ the thermal expansion coefficient, and $\mathbf{e}_z$ the unit vector in the *z*-direction. Additionally, for the top of the cylinder rotating with an angular velocity $\Omega$, we define the rotational Reynolds number as $Re = \Omega R^{*2}/\nu$. The boundary conditions are

at $r$=1 and $z$=0: $\quad v_r = v_\theta = v_z = 0, \qquad (4)$

at $z$=$A$: $\quad v_r = v_z = 0, \quad v_\theta = Re\, r, \qquad (5)$

$$T(r, z=0) = T(r, z=A) = 0,\ T(r=1, z) = 4z(1-z). \quad (6)$$

We study instability of steady axisymmetric flows $\{\mathbf{V}, P, T\}, \mathbf{V} = (U, V, W)$ with respect to infinitesimally small three-dimensional disturbances, which are decomposed into a Fourier series in the azimuthal direction and are represented as $\sum_{m=-\infty}^{m=+\infty}\{\tilde{\mathbf{v}}_m, \tilde{p}_m, \tilde{T}_m\} exp(\lambda t + m\theta)$, where $\lambda$ is a complex amplification rate, $\tilde{\mathbf{v}} = (\tilde{u}, \tilde{v}, \tilde{w})$, $\tilde{p}$ and $\tilde{T}$ are perturbation of the velocity, pressure, and temperature, respectively. The subscript $m$ denotes the $m$-th Fourier mode of a corresponding function. It is well-known that the linear stability problem separates for each $m$, which is an integer azimuthal wavenumber. Therefore, after an axisymmetric steady state is computed, solution of the stability problem is reduced to a series of 2D-like generalized eigenvalue problems defined for the eigenvalues $\lambda$ separately at different azimuthal wavenumbers $m$ (see, e.g., [14]). The steady flow is unstable when at least one $\lambda$ exists with a positive real part. The eigenvalue with the largest real part is called leading and parameters at which the leading eigenvalue crosses the imaginary axis are called critical.

To calculate steady states of Eqs. (1)-(7) and to study their linear stability with respect to three-dimensional infinitesimal disturbances, we use the finite volume discretization and the technique described and verified in [15]. The test calculations performed there showed that to keep critical parameters within 1% accuracy, one needs to apply at least 100 grid points in the shortest spatial direction. Note that our stability results for isothermal flow in a cylinder with a rotating top were successfully compared with several independent computations [15] and were validated experimentally [16]. The results for stability of convective flow in a side-heated cylinder are also well-compared with the independent result of [17]. Together with the convergence studies [14] these make us confident in the accuracy of the results reported below. In the following calculations, the size of the stretched finite volume grid varies from $N_r = 100$ to 300 points in the radial direction. The grid size in the axial direction is taken as $N_z = AN_r$. The grid size is chosen to ensure convergence to at least three correct decimal places in the calculated critical parameters.

## RESULTS

Figure 2 shows dependence of the critical Grashof number on the Prandtl number for three fixed values of the Reynolds number *Re*=0, 200 and 400. Due to difference in the critical values and in the qualitative behaviour of the curves, the graphs in Fig. 2 are divided into two frames for $Pr \le 1$ and for $Pr \ge 1$. We observe that the destabilization at small Prandtl numbers takes place starting from a certain, not very large, value of the Reynolds number (*Re*=400), while at smaller values (*Re*=200) the critical azimuthal modes replace each other at approximately the same values of the critical Grashof number. According to arguments given in [11], the destabilization at small Prandtl numbers is caused by mainly hydrodynamic mechanisms, such as interaction of counter rotating vortices and advection of angular momentum. To destabilize the base flow, these mechanisms must become strong enough, which happens at a sufficiently large value of the Reynolds number. An indication of the absence of the described destabilization effect is the appearance of the spoke pattern at non-zero *Re*. In Fig. 2a it is observed at *Re*=200 for *m*=5 and 6.

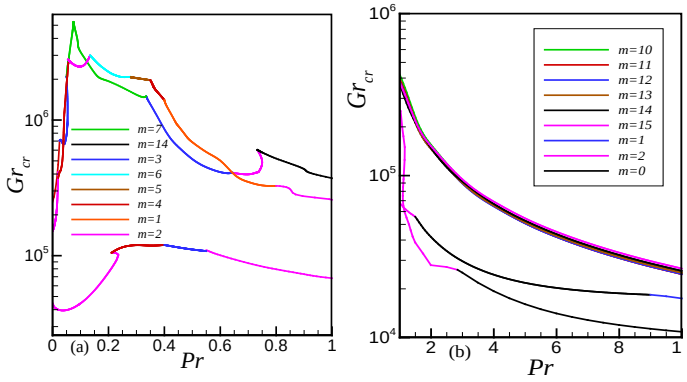


**Figure 2** Neutral stability curves $Gr_{cr}(Pr)$ for flow in a vertical cylinder with parabolic temperature profile at the sidewall and rotating top for fixed values of the Reynolds number *Re*=0, 200, and 400. Colors correspond to different critical Fourier modes $m_{cr}$.

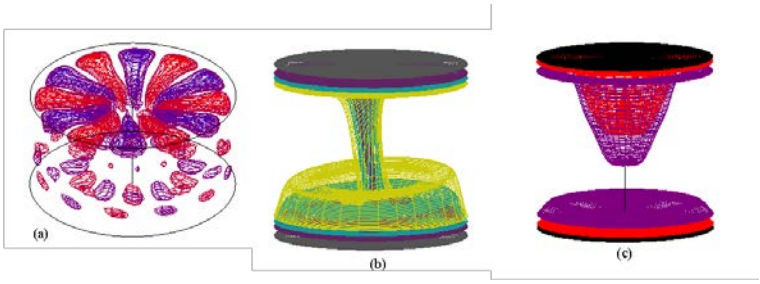


**Figure 3** Snapshots of isotherms corresponding to different instability modes observed at large Prandtl numbers. (a) spoke pattern *Pr*=0.3, $Gr=2.16\times10^6$, *Re*=200, (b) oscillating jet *Pr*=7, $Gr=2\times10^4$, *Re*=34.8, (c) cold plume (*Pr*=7, *Gr*=5820, *Re*=50).

At $Pr \ge 1$ the instability, as well as the destabilization, take place mainly due to the change of the temperature distribution. In the absence of rotation the instability sets in as a spoke pattern [18]. With the increase of rotation of the top the area with the most unstable stratification is shifted towards the axis, so that the spoke pattern is replaced by an "oscillating jet" [6] or by "cold plumes" [8]. This may happen at significantly smaller Reynolds numbers. In fact, for each *Pr* there exists a relatively low value of Reynolds number at which the effect is strongest, e.g. at $Re \approx 50$ in Fig. 1c. We observe also that for large Prandtl numbers the destabilization at *Re*=200 is stronger than that at *Re*=400. Note also that in the absence of rotation the instability results in a spoke pattern. The critical Grashof numbers at *Re*=0 are very close for $10 \le m \le 15$ (Fig. 2b). The oscillating jet and cold plumes modes are characterized by a smaller azimuthal wavenumber, which is seen on the curves corresponding to *Re*=200 and 400 in Fig. 2b. Examples of the

computed three instability modes are shown in Fig. 3 and some experimental observations are shown in Fig. 4.

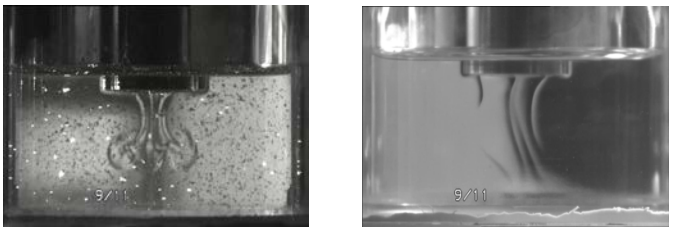

**Figure 4** Experimentally observed cold plume (left) and oscillating jet (right) instabilities. From Teitel et al. (2008). For more details and experimental videos see http://www.eng.tau.ac.il/~gelfgat/CZ_2007.htm

We illustrate the effect of stratification change on several examples corresponding to the neutral curve shown in Fig. 1c. In this case the spoke pattern instability observed for $0 \le Re < 30$ with $m_{cr}=10$ or 11 is replaced by another one, having $m_{cr}=1$ and exhibiting a steep decrease of the critical Grashof number from $Gr_{cr} \approx 2.5 \times 10^4$ at $Re \approx 30$ to $Gr_{cr} \approx 10^4$ at $Re \approx 47$. Note that this mode crosses the $Re=0$ axis at $Gr \approx 4.7 \times 10^4$, so that in the absence of rotation it is less unstable than the spoke pattern mode. At $Re \approx 47$ this mode is replaced again by the axisymmetric one ($m_{cr}=0$) that continues to even smaller values of $Gr$ reaching $Gr_{cr} \approx 3000$ at $Re \approx 51.5$ . With further increase of the Reynolds number the critical Grashof number slowly grows and several other mode switches take place.

Considering the first example of Fig. 5b we note that the striking feature of this case is the almost unchanged streamlines (not shown here) and slightly changed isotherm patterns corresponding to the zero and non-zero Reynolds numbers. The rotation is extremely slow, so that taking the characteristic length 10 cm and the viscosity of water $\approx 10^{-6}$ m$^2$/s, $Re \approx 35$ would correspond to approximately 0.2 rpm. It is really difficult to see what could change in the flow to so strongly affect its stability properties. One of possible explanations is the following. The temperature perturbation of the destabilized flow (not shown here) is located near the axis in the area of unstable temperature stratification and can be driven by the Rayleigh-Bénard instability mechanism. The spoke pattern instabilities also appear due to the Rayleigh-Bénard mechanism, but their disturbances are located mainly in the thinner unstable layer closer to the cylindrical wall [18]. The Rayleigh-Bénard driven instabilities located near the axis were also observed in the considered configuration without rotation, but in taller cylinders [12]. Therefore, we observe here two competing instability modes. The examination of isotherms (Fig. 5b) shows that while unstably stratified temperature near the sidewall is unaltered by the rotation, the temperature change along the axis slightly steepens, which is seen as a slight raise of a point where two upper isotherms arrive to the axis. In Fig. 5a the axial temperature gradient of flows at several critical points is compared with those calculated at the same Grashof numbers but with zero rotation rate. We observe that the axial gradients at the instability points are always slightly steeper than those corresponding to zero rotation cases.

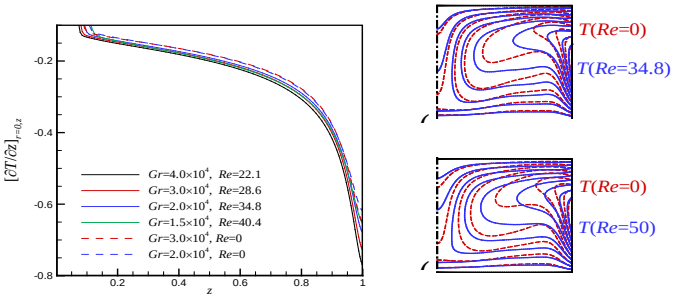


**Figure 5** (a) Axial temperature gradients for several flows at the critical points corresponding to the descending $m=1$ branch of Fig. 1c, and several flows at the zero rotation. (b,c) comparison of the isotherms pattern with and without slow rotation of the top boundary.

On the basis of the above, we can offer the following explanation of the observed destabilization. We assume that in a wide range of Grashof numbers the growth rate of the mode, leading at $Re \approx 35$, is negative but close to zero, so that this disturbance mode does not become unstable. A slow rotation of the upper boundary creates a small change in the base flow that makes the disturbance unstable. The rotation of the top slows down the axially directed radial flow along it. Consequently, the descending flow along the axis also slows down. As a result, the convective mixing near the axis reduces, which leads to steeper axial temperature gradients. When, with the increase of the Reynolds number, the unstable temperature gradient exceeds a certain critical average value the instability sets in. We observe that at larger Grashof numbers lower axial gradient is critical (0), which is quite expected and results from the dependence of the growth rate on the base flow. The three-dimensional unsteady temperature pattern that results from the above instability mode is illustrated in Fig. 2. We observe that the isosurfaces form a thin tube that rotates along the axis. Such an instability pattern was observed in experiments of [6,8], where it was called "cold jet" or "oscillatory jet" instability.

A light increase of the Reynolds number to $Re \approx 47$ leads to even stronger reduction of the critical Grashof number to $Gr_{cr}=5819$ (Fig. 1c). Again, we observe a steepening of the unstable temperature gradient (Fig. 4c) at the axis, which in this case leads to the so-called "cold thermals" instability (Fig. 2c), which is also of the Rayleigh-Bénard nature. Here the cold fluid is advected along the upper surface towards the axis where unstable stratification triggers the instability, appearing as a rapid descent of the cold fluid along the axis and oscillations of the main convective vortex.

The full description of model problem for the Czochralski flow that motivated this study can be found in [9,10]. The crucible radius is chosen as the characteristic length, and therefore definitions of the Grashof and Reynolds number remain unchanged. The flow is described by the Boussinesq equations (1)-(3) with no-slip boundary conditions at the

bottom and the sidewall of the crucible, while the temperature there is prescribed according to the experiment [7]

at $r = 1$: $v_r = v_\theta = v_z = 0, \quad T = 1$ (7)

at $z = 0$: $v_r = v_z = v_\theta = 0, \quad T = 0.8571 + 0.1429r^2$ (8)

The central part of the upper surface touches the rotating cold crystal dummy kept at the lower temperature. The remaining part of the upper surface is cooled by a convective flow of air above it and is subject to the thermocapillary force. This reads

at $z = A \; and \; r \leq \frac{R_{crystal}}{Rcrucible}$: $v_r = v_z = 0, v_\theta = Re_{crystal} r$ (9)

at $z = A \; and \; r > \frac{R_{crystal}}{Rcrucible}$: $v_z = 0,$

$$\frac{\partial v_r}{\partial z} = -MaPr\frac{\partial T}{\partial r}, \; \frac{\partial v_\theta}{\partial z} = -MaPr\frac{\partial T}{r\partial \theta} \quad (10)$$

The flow is driven by buoyancy, thermocapillarity and rotation, which are characterized by the Grashof, Marangoni and Reynolds numbers. The Marangoni number is defined as $Ma = \gamma \Delta T R/\nu\alpha$, where $\gamma = |d\sigma/dt|$ is assumed to be a constant and σ is the surface tension coefficient. The working liquid is $NaNO_3$ with *Pr*=9.2. Since both the Grashof and Marangoni numbers depend on the characteristic temperature difference we calculate *Ma*=586 Δ*T* /*Pr* and *Gr*=1.9×10$^5$Δ*T* and use Δ*T* as a critical parameter.

Figure 6 shows changes of the flow and perturbation patterns along the neutral stability curve of Fig. 1a. Since the instability in this case is axisymmetric ($m_{cr}$=0), we plot the stream function and its perturbation instead of the two meridional velocity components. As above, in the case of our characteristic problem at *Pr*=7, we observe that with the increase of rotation the main convective circulation weakens, which leads to a steepening of the axial unstable temperature gradient near the axis. This leads to strong temperature perturbations that develop below the cold crystals and descend with the flow along the axis. The snapshots of isotherms shown in Figs. 7 and 8 for the points *a* and *c* of 0a, respectively, show similar oscillations of cold thermals that descend along the axis. Examination of the case of [8] shown in 0b shows similar perturbation patterns and similar time-dependence. We conclude that the destabilization observed for the large Prandtl number Czochralski melt flow has the same nature as the one observed for the simplified characteristic problem. Rotation of the crystal causes a retardation of the main convective circulation, which leads to a formation of an unstably stratified layer beyond the crystal. This layer is destabilized by the Rayleigh-Bénard mechanism, which is mainly defined by the layer thickness. With the increase of the rotation rate (the Reynolds number) formation of the unstable layer takes place at a lower Grashof number, thus resulting in the destabilization of this convective flow by rotation.

## CONCLUDING REMARKS

We showed that a model problem of flow in a vertical cylinder with a parabolic temperature profile on the sidewall, isothermal top and bottom and rotating top resembles the destabilization of natural convection flow by a weak rotation, which recently was reported for different configurations of Czochralski model flow. Studying the mechanisms responsible for the destabilization we have found that at large Prandtl number the destabilization is caused by a development of an unstable stratification below the cold top boundary. A slow rotation of the top leads to a steepening of axial temperature gradient and further destabilization of the unstably stratified region. This, in its turn, causes a replacement of the spoke pattern eigenmode by another instability mechanism. The latter, depending on the rotation rate, appears to be either “oscillating jet” or “cold plume” instability, both observed in the Czochralski model flows.

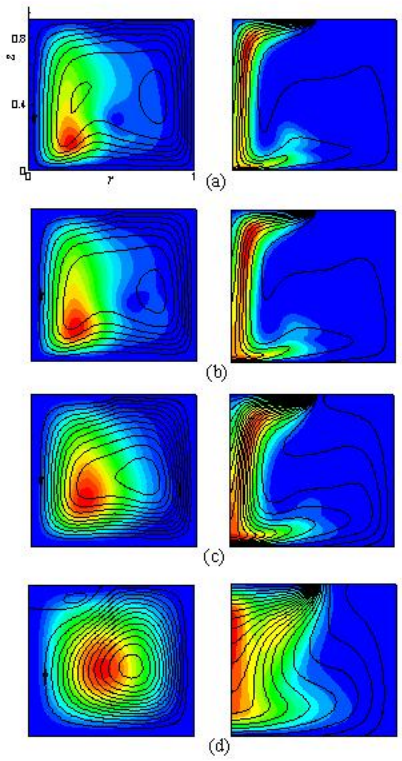


**Figure 6** Streamlines (left frames) and isotherms (right frames) shown by lines and perturbations of the stream function and temperature shown by color for four points a, b, c, and d shown in Fig. 1a. $m_{cr}$=0. (a) Δ*T*=0.63, *Re*=0, $\psi_{min}$=–1.38, (b) Δ*T*=0.37, *Re*=75, $\psi_{min}$=–1.22, (c) Δ*T*=0.1, *Re*=104, $\psi_{min}$=–0.81, (d) Δ*T*=0.018, *Re*=100, $\psi_{min}$=–0.40, $\psi_{max}$=–0.0066.


## ACKNOWLEDGEMENT

This study was supported by the German-Israeli Foundation, grant No. I-954 -34.10/2007. The author wishes to acknowledge fruitful discussions with to D. Schwabe, H. Wilke and E.Kit.

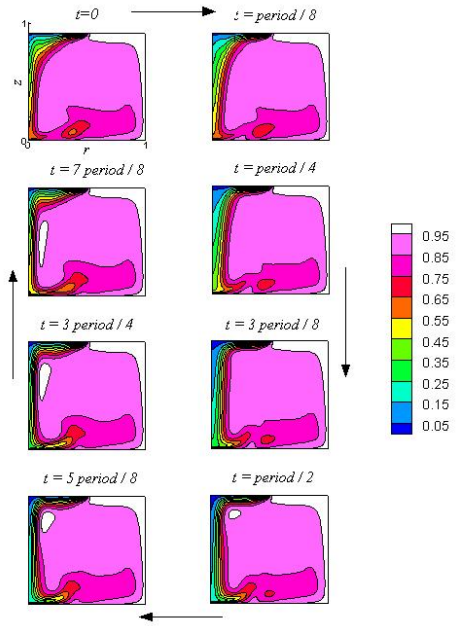


**Figure 7** Eight equally distanced snapshots of isotherms of supercritical oscillatory state during one period of oscillations. Flow in the Czochralski model of [10] top (Fig. 1a, point a) at $\Delta T=0.63$, $Re_{cr}=0$, $m_{cr}=0$.

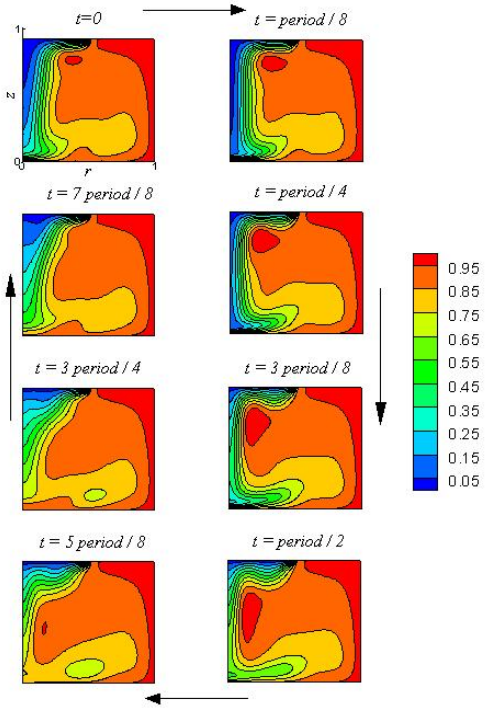


**Figure 8** Eight equally distanced snapshots of isotherms of supercritical oscillatory state during one period of oscillations. Flow in the czochralski model of [10] top (Fig. 1a, point a) at $\Delta T=0.1$, $Re_{cr}=100$, $m_{cr}=0$.

## REFERENCES


[1] Chandrasekhar S., *Hydrodynamic and Hydromagnetic Stability*. Oxford Univ. Press, 1961.

[2] Koschmieder E.L., *Bénard Cells and Taylor Vortices.* Cambridge University Press, 1993.

[3] Brummel N., Hart J.E., & Lopez J.M., On the flow induced by centrifugal buoyancy in a differentially-heated rotating cylinder. *Theoret. Comput. Fluid Dynamics*, Vol. 14, 2000, pp. 39-54.

[4] Ali M.E. and McFadden, G.B., Linear stability of cylindrical Couette flow in the convection regime, *Phys. Fluids*, Vol.17, 2005, 054112.

[5] Müller G., Review: The Czochralski Method - where we are 90 years after Jan Czochralski´s invention. *Crystal Research and Technology*, Vol. 42, 2007, pp. 1150-1161

[6] Hintz P., Schwabe D., and Wilke H., Convection in Czochralski crucible – Part I: non-rotating crystal, *J. Cryst. Growth*, Vol. 222, 2001, pp. 343-355.

[7] Schwabe D., Sumathi R.R., and Wilke H., An experimental and numerical effort to simulate the interface deflection of YAG, *J. Cryst. Growth*, Vol. 265, 2004, pp. 440-452.

[8] Teitel M., Schwabe D., and Gelfgat A.Yu., Experimental and computational study of flow instabilities in a model of Czochralski growth, *J. Cryst. Growth*, Vol. 310, 2008, pp. 1343-1348.

[9] Gelfgat A.Yu., Numerical Study of Three-Dimensional Instabilities of Czochralski Melt Flow Driven by Buoyancy Convection, Thermocapillarity and Rotation. *In: Studies of Flow Instabilities in Bulk Crystal Growth*, ed. A. Gelfgat, Transworld Research Network, 2007, pp. 57-82.

[10] Crnogorac N., Wilke H., Cliffe K. A., Gelfgat,A. Yu., and Kit E., Numerical modelling of instability and supercritical oscillatory states in a Czochralski model system of oxide melts, *Crystal Research and Technology*, Vol. 43, 2008, pp. 606-615.

[11] Gelfgat A.Yu., Destabilization of convection by weak rotation. *J. Fluid Mech.*, Vol. 385, 2011, pp. 377-412

[12] Gelfgat A.Yu., Bar-Yoseph P.Z., and Solan A., Axisymmetry breaking instabilities of natural convection in a vertical Bridgman growth configurations, *J. Cryst. Growth*, Vol. 220, 2000, pp. 316-325.

[13] Gelfgat A.Yu., Bar-Yoseph P.Z., and Solan A., Three-dimensional instability of axisymmetric flow in a rotating lid - cylinder enclosure, *J. Fluid Mech.*, Vol. 438, 2001, pp. 363-377.

[14] Gelfgat A.Yu., Three-dimensional instability of axisymmetric flows: solution of benchmark problems by a low-order finite volume method, *Int. J. Numer. Meths. Fluids*, Vol. 54, 2007, pp. 269-294.

[15] Gelfgat A.Yu., Three-dimensionality of trajectories of experimental tracers in a steady axisymmetric swirling flow: effect of density mismatch, *Theoret. Comput. Fluid Dyn.*, Vol. 16, 2002, pp. 29-41.

[16] Sørensen J.N., Naumov I., and Mikkelsen R., Experimental investigation of three-dimensional flow instabilities in a rotating lid-driven cavity. *Exp. Fluids*, Vol. 41, 2006, pp. 425-440.

[17] Gemeny L.E., Martin Witkowski L., and Walker J.S., Buoyant instability in a laterally heated vertical cylinder. *Int. J. Heat Mass Transf.*, Vol. 50, 2007, pp. 1010-1017.

[18] Gelfgat A.Yu., Bar-Yoseph P.Z., Solan A., and Kowalewski T., An axisymmetry- breaking instability in axially symmetric natural convection, *International Journal of Transport Phenomena*, Vol. 1, 1999, pp. 173-190.